Precision Engineering 33 (2009) 150–159

Contents lists available at ScienceDirect

Precision Engineering

journal homepage: www.elsevier.com/locate/precision

Modeling high-temperature glass molding process by coupling heat transfer and viscous deformation analysis

Jiwang Yan[a,*], Tianfeng Zhou[a], Jun Masuda[b], Tsunemoto Kuriyagawa[a]

[a] Department of Nanomechanics, Graduate School of Engineering, Tohoku University, Aoba 6-6-01, Aramaki, Aoba-ku, Sendai 980-8579, Japan
[b] Toshiba Machine Co., Ltd., 2068-3, Ooka, Numazu-shi, Shizuoka-ken 410-8510, Japan

ARTICLE INFO

Article history:
Received 29 November 2007
Received in revised form 24 March 2008
Accepted 9 May 2008
Available online 5 July 2008

Keywords:
Glass
Press molding
Optical element
Thermo-mechanical property
Viscosity
Finite element method

ABSTRACT

Glass molding is as an effective approach to produce precision micro optical elements with complex shapes at high production efficiency. Since glass is deformed at a high temperature where the mechanical and optical properties depend strongly on temperature, modeling the heat transfer and high-temperature deformation behavior of glass is an important issue. In this paper, a two-step pressing process is proposed according to the non-linear thermal expansion characteristics of glass. Heat transfer phenomenon was modeled by considering the temperature dependence of specific heat and thermal conductivity of glass. Viscosity of glass near the softening point was measured by uniaxially pressing cylindrical glass preforms between a pair of flat molds using an ultraprecision glass molding machine. Based on the numerical models and experimentally measured glass property, thermo-mechanical finite element method simulation of temperature rise during heating and material flow during pressing was carried out. The minimum heating time and pressing load changes were successfully predicted.

© 2008 Elsevier Inc. All rights reserved.

1. Introduction

Glass lens has many predominant advantages over the plastic counterpart on aspects of hardness, refractive index, light permeability, stability to environmental changes in terms of temperature and humidity, and so on. For this reason, glass lenses have been demanded increasingly in the field of high-resolution digital cameras, mobile phone cameras, and CD/DVD players and recorders. Conventionally, glass lenses have been fabricated by a series of material removal processes, such as grinding, lapping and polishing, which requires a long production cycle and results in a very high production cost [1,2]. As an alternative approach, glass molding process has been accepted as a promising way to efficiently produce precision optical elements with complex shapes, such as aspherical lenses, Fresnel lenses, diffractive optical elements (DOEs), micro lens arrays, and so on [3,4].

According to thermal cycle, a typical glass molding process can be divided into four stages: heating, pressing, annealing and cooling, which are schematically shown in Fig. 1. Firstly, a glass preform is placed on the lower mold, and inert gas, such as nitrogen (N_2), is flowed to purge the air in the machine chamber; then the molds and glass preform are heated to the molding temperature by a heat source, such as infrared lamps (Fig. 1(a)). Secondly, the glass preform is pressed by closing the two mold halves (Fig. 1(b)). Thirdly, while a small pressing load is maintained, the formed lens is slowly cooled down to release the internal stress, namely, annealing (Fig. 1(c)). Finally, the glass lens is cooled rapidly to ambient temperature and released from the molds (Fig. 1(d)). Through these four stages, the shapes of the mold cores are precisely replicated to the glass lens.

Glass is a strongly temperature-dependent material. At room temperature, glass is a highly hard and brittle material; at a high temperature, however, it becomes a viscoelastic body or a viscous liquid. Thermal expansion of glass is also significant. For example, the volume–temperature relationship of a commonly used glass L-BAL42 (Ohara Corp., Kanagawa, Japan) is plotted in Fig. 2. Softening point (SP) is defined as the temperature at which the glass deforms under its own weight and behaves as liquid. Yielding point (A_t), also called "deformation point", is a temperature at which glass reaches its maximum expansion and a relatively low plasticity and starts shrinking. When such a melt is gradually cooled, the volume decreases abruptly down to a transition temperature (T_g) below which volume shrinkage occurs at a slower rate. Pressing of a glass lens is always performed above T_g. Annealing point (AP) is the upper end of the annealing range for the pressed glass lens, at which the internal stress is reduced to a practically acceptable value over a short period. Strain point (StP) represents the lower end of the annealing temperature range. It is also the upper limit of

* Corresponding author. Tel.: +81 22 795 6946; fax: +81 22 795 7027.
E-mail address: yanjw@pm.mech.tohoku.ac.jp (J. Yan).

0141-6359/$ – see front matter © 2008 Elsevier Inc. All rights reserved.
doi:10.1016/j.precisioneng.2008.05.005

Downloaded from Yan Laboratory, Keio University at http://www.yan.mech.keio.ac.jp. Redistribution is subject to copyright licence from the journal publisher.

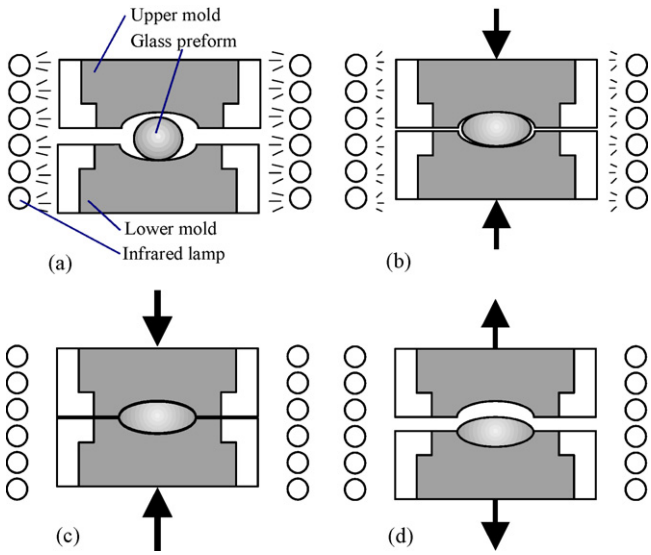

Fig. 1. Schematics of four stages of a glass lens molding process: (a) heating, (b) pressing, (c) annealing and (d) cooling.

service temperature of a glass component. During annealing, glass is slowly cooled down from AP to somewhat below StP.

Determination of a suitable temperature for pressing is an essential issue for glass molding. If pressing is performed above A_t and held on to keep the shape of the lens during cooling, the volume expansion around A_t will lead to a sharp increase in pressing load, and in turn, adhesion of glass to molds [5]. On the contrary, if pressing is done below A_t, a high pressing load will be required because glass is not sufficiently softened at this temperature range. In this case, significant residual stresses will occur in the glass lens, and the high pressing load may also shorten the service life of the molds. This problem is a critical one especially when molding micro Fresnel lenses and DOEs where the molds have extremely fine grooves on the surface. A high pressing load may cause deformation and damages to the micro grooves.

To solve this problem, in this work, we proposed a two-step pressing method. The first pressing step is done at a high temperature near the softening point (SP), so that glass behaves as a viscous liquid and most of material deformation can be achieved at a low load. After the first step, the pressing load is reduced and

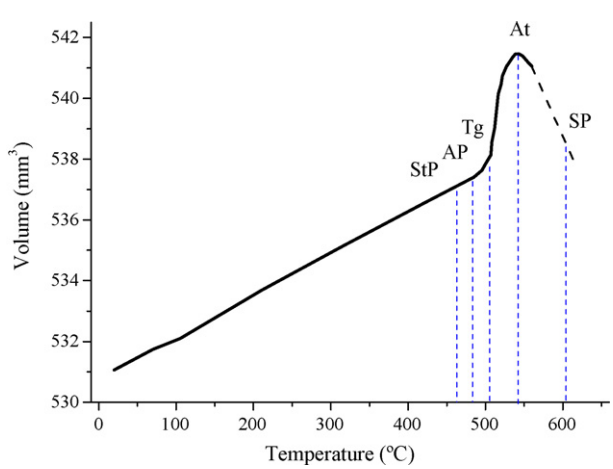

Fig. 2. Plot of volume change against temperature for a typical optical glass L-BAL42, showing strongly temperature-dependent thermal expansion characteristics. SP, softening point; A_t, yielding point; T_g, transition point; AP, annealing point; StP, strain point.

the temperature is lowered to be between T_g and A_t. Then the second pressing is done at this temperature to close the molds and obtain the final shape of the lens. The two-step pressing method can achieve both high lens accuracy and long mold life. Another advantage of this method is that the thermal expansion coefficient of glass is approximately linear below T_g, so that it is easy to calculate the compensation profile of the molds according to the objective shape of the lens. The two-step pressing method is especially effective for molding Fresnel lenses, DOEs and other surface microstructures.

In the first pressing step, two issues are practically important: one is to make clear the thermo-mechanical properties of glass at a temperature near SP, and the other is to uniformly heat the whole glass to this temperature. If temperature distribution in glass is not uniform, thermo-induced disorder of optical properties may occur. Overheating should also be avoided to prevent the molten glass from adhering to mold surfaces. Therefore, modeling of heating process and determination of heating time is essential for improving both product accuracy and manufacturing efficiency [6].

Since glass is transparent in infrared light, it cannot be directly heated by the infrared lamp, but instead, has to be indirectly heated by the molds and the surrounding gas. Therefore, heat transfer in this case involves heat conduction, heat convection and radiation. Also, heat expansion coefficient, heat conductivity, heat capacity and other parameters of glass are also changing with temperature. From these aspects, the heat transfer in glass molding is a very complicated issue. However, at present, precise measurement of the heat transfer in a glass lens is still difficult, although Field and Viskanta [7] demonstrated the possibility of experimental measurement of temperature distributions in soda-lime glass plates.

Finite element method (FEM) has shown to be an effective approach to simulate a forming process and visualize the heat transfer in glass. For example, Wilson et al. [8] studied the heat transfer across tool-workpiece interface by using an FEM code, DEFORM^{TM}-2D. Viskanata and Lim [9] proposed a physical model for internal heat transfer in glass and heat exchange across glass-mold interface in one dimension. Yi and Jain [10] applied DEFORM^{TM}-2D to the simulation of aspherical glass lens molding. However, most of these studies analyzed the heating process by separately considering heat transfer and glass deformation. The numerical models they used did not take into account the time-dependent and temperature-dependent changes of thermal and mechanical properties of glass, which might cause considerable simulation errors. To date, there is no available literature on the dynamic modeling of a high-temperature glass forming process by comprehensively considering the heat transfer and the thermal deformation of glass. Therefore, precise prediction of process parameters, such as heating time and pressing load is still difficult.

The objective of the present study is to establish a series of thermo-mechanical models for the glass molding process, from heating, pressing, annealing to cooling, to enable FEM simulation and visualization of the process and accurate prediction of optimal process parameters. It is expected that the theoretical work can partially reduce the number of trial-and-error experiments and provide deterministic criteria for active compensation of the mold geometry. In the present paper, firstly, thermal phenomenon during the glass molding process was analyzed by considering heat transfer within glass and at the interface among glass, molds and surrounding gas environment. Secondly, the high-temperature viscosity of glass near the softening point SP was measured using an ultraprecision glass molding machine by uniaxially press cylindrical glass preforms between a pair of flat molds. Thirdly, the developed numerical models and the measured viscosity properties were incorporated into coupled thermo-mechanical FEM simulation of the glass pressing process based on a viscous fluid model. Through a comparison between the experimental results

Table 1
Thermal expansion characteristics of glass L-BAL42

Characteristic point in the volume–temperature curve	Temperature (°C)
Strain point (StP)	476
Annealing point (AP)	494
Transition temperature (T_g)	506
Yielding temperature (A_t)	538
Softening point (SP)	607

and the simulated results in terms of minimum heating time and pressing load changes, it will be shown that the developed thermal and mechanical models can be used to precisely predict important process parameters of glass molding.

2. Theoretical models

2.1. Thermal expansion of glass

Thermal expansion is an important issue in lens molding because it greatly influences the form accuracy of the lens. As shown in Fig. 2, the thermal expansion of glass is strongly temperature-dependent. The expansion coefficient is approximately linear at low temperature (below T_g), and becomes non-linear in the high-temperature range. The thermal expansion coefficient increases significantly from T_g to A_t, then a negative expansion (namely contraction) occurs above A_t [11]. Ohlberg and Woo [12] proposed a complicated formula to describe the change of glass expansion coefficient, but it is still hard to precisely describe the thermal expansion coefficient in a single function. For simplification, linear approximations are adopted to represent the changes of thermal expansion coefficient in different temperature ranges.

To begin with, we consider the one-dimensional thermal expansion problem. The linear thermal expansion coefficient (α) can be given by Eq. (1):

$$\alpha = \frac{1}{l} \times \frac{\mathrm{d}l}{\mathrm{d}T} = \begin{cases} a_0 & -30 \le T < 70 \\ a_1 & 70 \le T < T_g \\ a_1 + a_2(T - T_g) & T_g \le T < A_t \end{cases} \quad (1)$$

where l is the overall length of material in the direction being measured; T is the instantaneous temperature in °C; a_0 is the constant thermal expansion coefficient in the working temperature range of glass; a_1 is the constant thermal expansion coefficient below T_g; and a_2 is the average gradient of the increase of thermal expansion coefficient between T_g and A_t. The glass material used in the present work is L-BAL42, the thermal characteristics of which are listed in Table 1. Other glasses show similar general trends in the volume–temperature curves. According to the data provided by the glass manufacturer, we obtain that $a_0 = 7.2 \times 10^{-6}$ l/°C, $a_1 = 8.8 \times 10^{-6}$ l/°C, and $a_2 = 3.0 \times 10^{-8}$ l/°C^2 in Eq. (1).

Next, we consider volume expansion in three-dimensional glass molding. The volume thermal expansion coefficient (β) is approximately three times the linear thermal expansion coefficient, thus it can be defined by Eq. (2). The temperature-dependent volume ($V(T)$) can then be calculated using Eq. (3).

$$\beta \approx 3\alpha \quad (2)$$

$$V(T) = V_0\left(1 + \int_0^T \beta\,\mathrm{d}T\right) = V_0\left(1 + 3\int_0^T \alpha\,\mathrm{d}T\right) = V_0 + \Delta V \quad (3)$$

where V_0 is the volume of glass at the reference temperature (0 °C), and ΔV is the swelling increment in volume after heating to temperature T. In the FEM simulation of molding process in this study, a module was activated to restore the volume change due to thermal expansion during remeshing, and the coefficient of thermal expansion was used to define the volumetric strain due to temperature changes.

2.2. Heat transfer models

On most occasions, glass molding processes are based on the "isothermal molding" method where pressing is performed after the glass preform reaches the same temperature as the molds. However, due to the fact that the heat absorption rate of glass is distinctly different from that of the mold materials, such as tungsten carbide (WC), silicon carbide (SiC), titanium carbide (TiC), nickel–phosphorous (NiP) plated steels and other alloys, even the glass preform and the molds are heated together by the same infrared lamp, there is a significant delay of temperature rise within the glass preform. Most of the heat transferred to the glass preform is from the lower mold and surrounding nitrogen during the soaking time. However, it is difficult to directly measure the temperature change in the glass preform even if the temperature of the molds can be easily monitored by thermocouples. Therefore, modeling of heat transfer phenomenon in glass molding is very important for working out heat balance.

Initially, we consider the heat transfer within a glass preform. The governing equation for heat conduction within an incompressible glass material is given by Eq. (4):

$$\rho C_p \frac{\partial T}{\partial t} = k\nabla^2 T \quad (4)$$

where ρ is the density; C_p is the specific heat; k is the thermal conductivity of glass; and t is the heating time. Most of the previous work on simulation of glass molding and other forming processes treated the specific capacity C_p and thermal conductivity k as constants [13,14]. However, in fact these two parameters are temperature-dependent, as experimentally demonstrated by early researchers [15,16].

As glass is a compound material, the specific heat of glass is known to vary with its composition and temperature. An empirical equation, namely, Sharp–Ginther equation [17], has been proposed to express the mean specific heat (C_m) of glass, as shown in Eq. (5).

$$C_m = \frac{a_3 T + C_0}{0.00146T + 1} \times 4.186 \times 10^3 \quad (5)$$

where a_3 is a constant of a glass material; C_0 is the true specific heat at 0 °C; and T is the temperature in °C. a_3 and C_0 are both decided by the glass compositions. This equation can be applied to a wide temperature range and has been widely used by later researchers.

The composition percentages of the glass samples offered by the glass manufacturer are shown in Table 2. An intermediate value of each composition was used to calculate the constants a_3 and C_0 in Eq. (5). According to the method described in reference [17], the calculated values were $a_3 = 0.000408$ J/°C^2 and $C_0 = 0.144$ J/°C, respectively. It was reported that oxides BaO and ZnO influence the thermal properties of glass [18]. However, from experimental results in the present study, we could not find obvious change of heat capacity due to BaO and ZnO so that we ignored their effects in this paper.

Table 2
Composition ratio of glass L-BAL42

Glass composition	Content (wt%)
SiO_2	40–50 (≈45)
BaO	20–30 (≈25)
B_2O_3	2–10 (≈6)
Al_2O_3	2–10 (≈6)
ZnO	2–10 (≈6)
Others	0–2 (≈2)

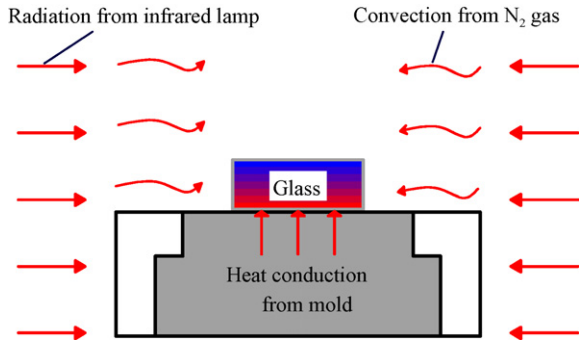

Fig. 3. Schematic presentation of heat transfer phenomenon during heating process.

The true specific heat C_p in Eq. (4) then can be easily calculated from the differential equation as follows:

$$C_p = \frac{d(TC_m)}{dT} \tag{6}$$

In Eq. (4), the thermal conductivity k is a variable of temperature in a complex manner due to the effects of high-temperature radiation. For simplicity, many investigators treated the high-temperature irradiation in glass as an equivalent thermal conductivity problem, and a temperature-dependent thermal conductivity ($k(T)$) was proposed for glass materials by Mann et al. [19]. In this work, based on the glass property data provided by the manufacturer, a modified formula is given in Eq. (7) to represent the thermal conductivity of glass L-BAL42.

$$k(T) = 1.028 + 0.000624T \tag{7}$$

Next, we consider the heat transfer from the mold and the nitrogen environment to the glass preform. As shown in Fig. 3, conduction, convection and radiation are three basic modes of heat transfer. In glass molding, thermal conduction at the glass-mold interface and thermal convection between the glass preform and the flowing nitrogen gas are primary contributions to the temperature rise of glass preform. The effect of infrared irradiation on glass is insignificant so that usually it can be ignored, although McGraw [20] proved that the effect of radiation on the temperature distribution within glass can be described by equivalent thermal conductivity.

The thermal boundary conditions of the glass preform during heating can be given by Eq. (8):

$$\begin{aligned} -k\frac{\partial T}{\partial n} &= h_M(T - T_M) \\ -k\frac{\partial T}{\partial n} &= h_N(T - T_N) \end{aligned} \tag{8}$$

where h_M is the interface heat transfer coefficient between the mold and glass; h_N is the heat transfer coefficient between the surrounding nitrogen gas and glass; T_M and T_N are the temperatures of the mold and the nitrogen gas, respectively. In Eq. (8), h_M is a function of interface pressure, thickness of air gap, amount of sliding, interface temperature, etc., and h_N is affected by chamber geometry, gas blowing velocity, flowing direction and so on. Therefore, strictly speaking, h_M and h_N are both variables. However, precise measurement of the changes of these coefficients is technically impossible under the present conditions. In this work, like in most of the previous studies [10], constant values of h_M (2800 W/(m^2 K)) and h_N (20 W/(m^2 K)) are assigned in the FEM simulation.

2.3. High-temperature viscosity of glass

When temperature is below T_g, glass is deemed as solid, which can be treated as a rigid or rigid-plastic material. However, when temperature is above the softening point SP, glass becomes a viscous liquid which is soft and flowable. Between T_g and SP, the properties of glass change greatly with temperature and it behaves as a viscoelastic/plastic body. In the two-step pressing process, to achieve glass deformation at a low load, the first press is performed near the softening point SP where glass can be approximately treated as a viscous Newtonian fluid.

High-temperature viscosity (η') is conventionally measured by parallel-plate viscometers according to Eq. (9), as reported by Gent [21].

$$\eta' = \frac{2\pi F h^5}{3V\dot{h}(2\pi h^3 + V)} \tag{9}$$

where F is the pressing load; h is the instantaneous height of the cylindrical glass sample; $\dot{h}$ is the axial deformation rate; and V is the volume of the sample. In the present work, instead of a parallel-plate viscometer, we used an ultraprecision molding machine to measure the viscosity of glass. Two flat molds were used as the rigid parallel-plate pair. Pressing load, displacement and speed were recorded by a load cell and a sensing-control system equipped in the machine.

During pressing, glass is assumed to be incompressible. However, due to thermal expansion as mentioned in Section 2.1, the volume of glass will change. To improve the accuracy of viscosity measurement, Meister [22] attempted to make modifications to Eq. (9) by considering the thermal expansion. Unfortunately, he made a mistake during formula deduction, which made the modified formula unreliable. In this work, we corrected the formula deduction process as shown in Eq. (10).

$$\begin{aligned} \eta &= \frac{2\pi F(h+\Delta h)^5}{3(V+\Delta V)\dot{h}[2\pi(h+\Delta h)^3 + V + \Delta V]} \\ &= \frac{2\pi F h^5(1+\alpha T)^5}{3V(1+3\alpha T)\dot{h}[2\pi h^3(1+\alpha T)^3 + V(1+3\alpha T)]} \\ &\approx \frac{(1+\alpha T)^5}{(1+3\alpha T)^2}\eta' \approx \frac{1+5\alpha T}{1+6\alpha T}\eta' \end{aligned} \tag{10}$$

where η is the modified value of viscosity, and Δh is the swelling increment in height.

After the glass viscosity at certain temperature intervals have been experimentally measured, the viscosity between these temperature intervals can be estimated by curve fitting. The function usually used for fitting glass viscosity is the Vogel–Fulcher–Tamman (VFT) equation as shown below [23,24].

$$\log \eta = A + \left[\frac{B}{(T - T_0)}\right] \tag{11}$$

where A, B, and T_0 are constants.

2.4. Stress–strain relationship in viscous deformation

Usually, bulk glass deformation behavior at a low strain rate above yielding point A_t has been modeled by the Newtonian incompressible law [25], described in terms of equivalent stress σ and strain rate $\dot{\varepsilon}$ as given by Eq. (12).

$$\sigma = 3\eta\dot{\varepsilon} \tag{12}$$

where η is the viscosity of glass, which can be obtained by the VFT equation as mentioned in Section 2.3. However, Chang et al. [26] found that flow stress function did not follow the exact Newton's Law for fluids and revised it by modifying the exponent of strain rate based on their experimental results. Similar phenomenon was observed in the present work. According to the properties of L-

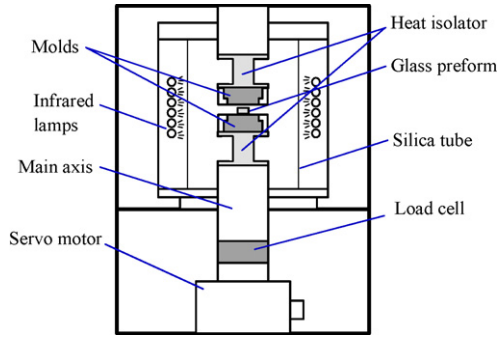

Fig. 4. Schematic diagram of the structure of the ultraprecision glass molding machine.

BAL42 glass, a modified flow equation was adopted as Eq. (13) in the FEM simulation.

$$\sigma = 3\eta\dot{\varepsilon}^{1.2} + 0.3 \tag{13}$$

It should be mentioned that during pressing, the heat transfer still continues. In this case, heat transfers to the glass preform from both the upper and lower molds. However, if the glass preform has been soaked enough so that a uniform temperature distribution is achieved within the glass preform during the heating stage, heat transfer during pressing will be insignificant and will not affect the constants in Eq. (13).

The frictional force between glass and molds during pressing was modeled as a constant shear friction [27], which can be defined by Eq. (14).

$$f_s = m\tau \tag{14}$$

where f_s is the frictional stress, τ the shear yield stress, and m is the friction factor. In this study, a value of 1.0 was assigned to m, assuming complete sticking between glass and molds without slip. Under this condition, the friction stress is a function of the yield stress of the deforming glass.

3. Viscosity measurement experiments

Experiments were carried out on an ultraprecision glass molding machine GMP211 (Toshiba Corp., Shizuoka, Japan), the structure of which is schematically shown in Fig. 4. In order to measure the high-temperature viscosity of glass by the parallel-plate method, a pair of flat molds made of tungsten carbide (WC) with surface coatings was used to press cylindrical glass preforms (basal diameter 12 mm, height 4.7 mm). The thermo-mechanical properties of the glass material are listed in Table 3. Nitrogen gas was used to purge the air to prevent the molds from oxidation at high temperatures. The molding chamber was covered by a transparent silica glass tube which can let the infrared rays in and separate the nitrogen gas from the air outside. Temperatures of the upper and lower molds are monitored by two thermocouples beneath the mold surfaces with a measurement accuracy of ±1 °C. The upper mold is remained stationary, while the lower mold is driven upward and downward by an AC servomotor with a resolution of 0.1 μm. A load cell is placed beneath the main axis to measure and feedback the pressing load with a resolution of 0.98 N.

Table 3
Thermo-mechanical properties of glass L-BAL42 at room temperature

Property	Value
Thermal expansion α ($\times 10^{-6}$/°C)	7.2
Thermal conductivity k (W/(m K))	1.028
Specific gravity d	3.05
Module of elasticity E ($\times 10^8$ N/m^2)	891
Module of rigidity G ($\times 10^8$ N/m^2)	357
Poisson's ratio ν	0.247

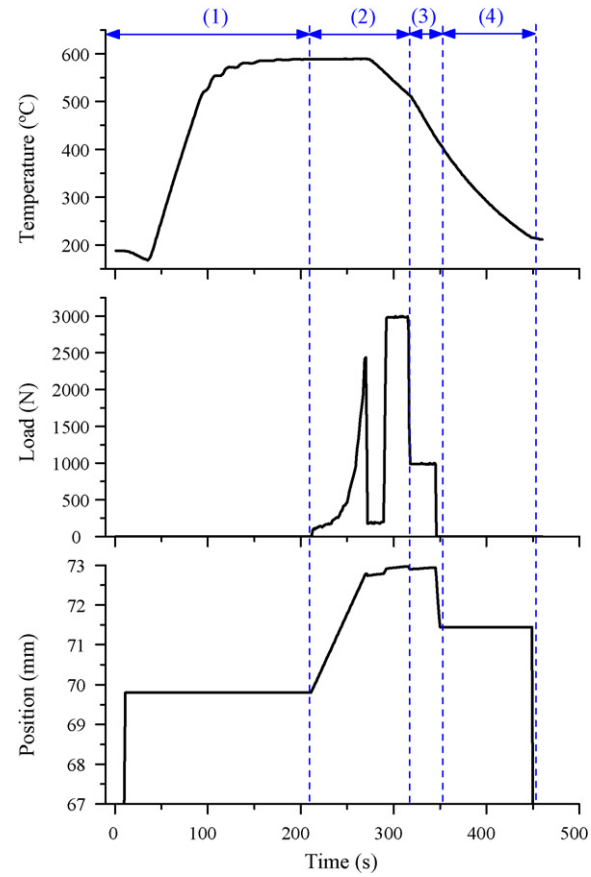

Fig. 5. Time sequences of temperature, pressing load and lower mold position during a molding cycle.

The four-stage molding process as shown in Fig. 1 was realized by a G-code computer program. During experiments, the temperatures of the upper and lower molds, the position of the lower mold, the pressing load applied to the molds were recorded, respectively, as functions of time. A series of typical time sequences of temperature, pressing load and lower mold position are plotted in Fig. 5. The operation procedures and corresponding conditions are outlined as follows:

(1) Putting a glass preform on the lower mold and raising the lower mold to position Z_1. Heating the molds and glass preform by the infrared lamps to the specified temperature (590 °C) above T_g at a heating rate of 3.6 °C/s, then keeping the specified temperature for soakage in the glass preform.
(2) Pressing the glass preform by moving the lower mold upwards in a constant pressing rate (3 mm/min) in the speed control mode until the pressing load reaches the first specified value (P_1 = 2500 N), and then keeping the press load constant until the position of the lower mold reaches the specified position Z_2. This is the first pressing step. After this step, moving the lower mold downward to remove the pressing load, and flowing the nitrogen gas to slightly cool the glass to below A_t, then performing the second press to close the molds at the second specified load (P_2 = 3000 N).
(3) Annealing the formed lens under a lower pressing load (P_3 = 1000 N) at a cooling rate of 1.4 °C/s until the temperature is reduced to 500 °C.

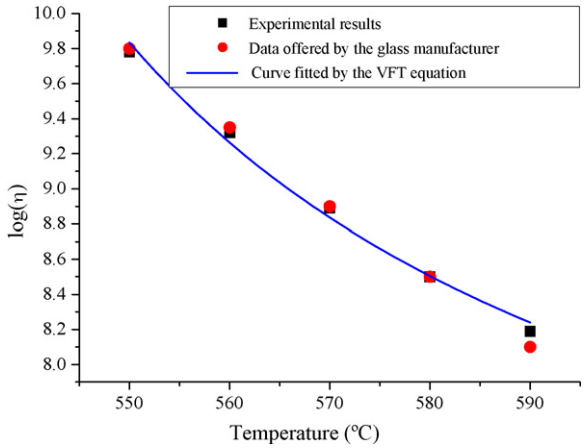

Fig. 6. Plot of glass viscosity against temperature near the softening point.

(4) Cooling the molded lens to 220 °C at a cooling rate of 2.0 °C/s.
(5) Releasing the molded glass and cooling it to room temperature (23 °C) naturally.

During the first pressing in step (2), the changes of the position of the lower mold and the pressing load were recorded and the data were processed using Eqs. (9) and (10), and the viscosity of the glass preform was obtained. The measured viscosity of glass is plotted against temperature in Fig. 6. A very good agreement can be seen between the results from the present study and those measured by the glass manufacture using a traditional parallel-plate viscometer. In the figure, the solid line is the fitted curve by the VFT equation using parameters $A = 5.87$, $B = 234.6$, $T_0 = 490$. Fig. 7(a) is a photograph of a cylindrical glass preform before experiment and Fig. 7(b) shows the deformed glass piece after experiments. The basal diameter and the thickness have been changed to 17.6 and 2.2 mm, respectively.

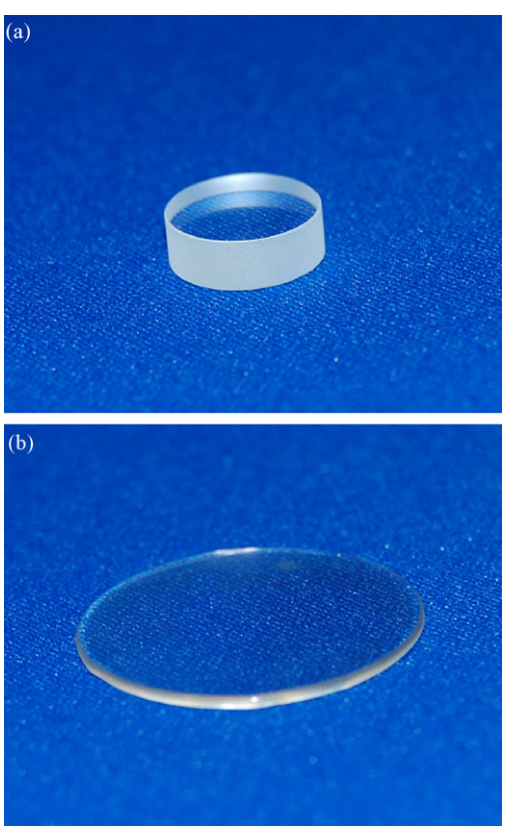

Fig. 7. Photographs of (a) a cylindrical glass preform before experiments and (b) press molded flat piece.

4. FEM simulations

Computer simulations of the glass molding process were carried out using a commercially available FEM program DEFORM™-3D. The program is capable of simulating large deformation of material flow under isothermal and non-isothermal conditions [28,29]. The FEM model is shown in Fig. 8. In the model, the two molds are assumed as completely rigid bodies; the glass preform is deformable and becomes a Newtonian fluid at the pressing temperature. Two-dimensional rigid wall boundaries are used for the upper mold, and one-dimensional rigid wall boundaries are set to the lower mold. The glass preform is totally free of constraints except its surface contact with the two molds. In order to save computation time and improve simulation accuracy, calculation was done for one-fourth of the cylindrical glass preform by taking advantage of the geometrical symmetry. The element remeshing was updated automatically based on an optimized Lagrangian scheme. The numerical models and boundary conditions presented in Section 2 and the experimentally measured results of glass viscosity in Section 3 were incorporated into the FEM simulation, which enabled a coupled thermal–mechanical analysis.

To start the simulation, the mold was heated from the room temperature to the pressing temperature (590 °C); after pressing, annealing and cooling, the first molding cycle was finished at a temperature of 220 °C. From the second molding cycle, the starting temperature was 220 °C. This temperature cycle is the same as that of an actual molding process. In simulation, the temperature distribution within the molds was assumed to be uniform. The temperature of the lower mold measured by the thermal couple was used as the temperature boundary condition of the mold. Fig. 9 shows temperature distributions in the glass preform during heating. After heating for 120 s, the temperature of the bottom surface was 66 °C higher than that of the top surface (Fig. 9(a)). The temperature difference was decreased to 10 °C after heating for 180 s (Fig. 9(b)). Then, after heating for 220 s, the temperature became uniform within the whole glass preform and reached the pressing

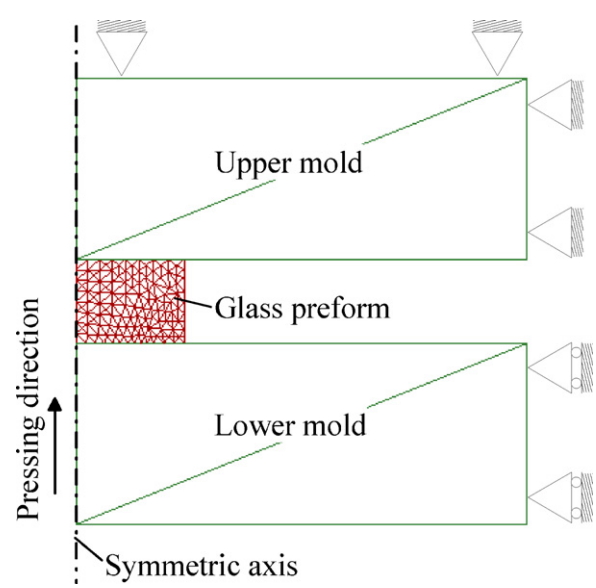

Fig. 8. FEM simulation model for glass molding tests using flat molds.

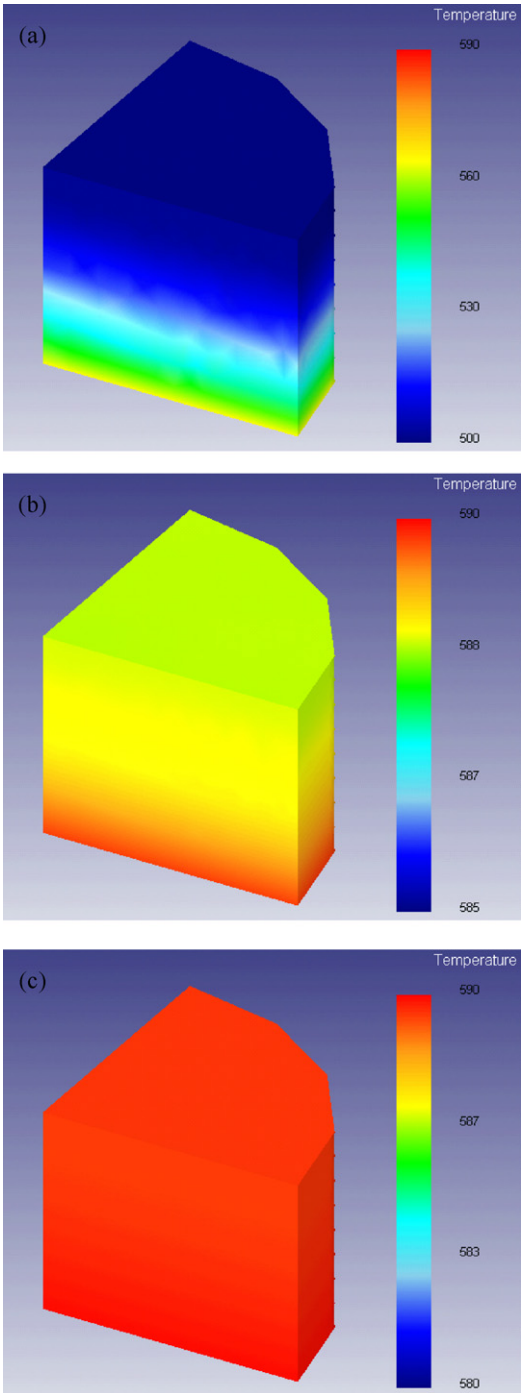

Fig. 9. Temperature distributions in the glass preform at different heating time: (a) 120 s, (b) 180 s, and (c) 220 s.

temperature 590 °C (Fig. 9(c)). The simulation results of the temperature rises on the bottom and the top surfaces of the glass preform during the heating process are plotted in Fig. 10. For comparison, the experiments results of temperature changes of the lower mold are also plotted in the figure.

Heating time determines the uniformity of temperature in glass, and affects the pressing load too. We define a "minimum heating time" which is the time span from the start of heating to the moment that the whole glass preform has reached the molding temperature (590 °C) uniformly. From the temperature-dependence of viscosity, we can assume that the minimum heating

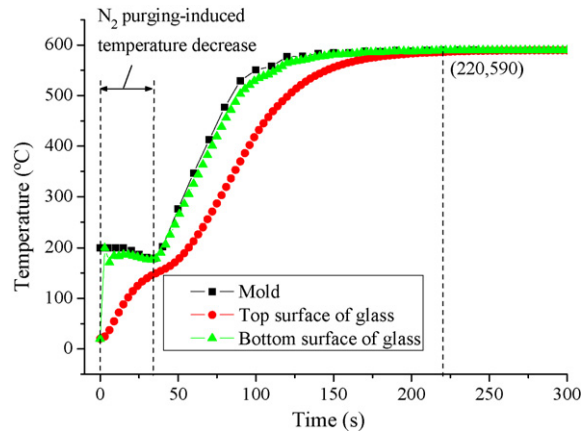

Fig. 10. Temperature rises of the mold and the upper/lower surfaces of glass during heating.

time is the shortest time for getting the lowest pressing force. Even if heating continues after the minimum heating time, the rising rate of pressing load will not decrease further. To verify this effect, experimentally measured pressing loads after different heating time are plotted against the displacement of lower mold in Fig. 11. It can be seen that after 180 s heating, there is a sharp increase in pressing load at the early stage; while after heating for longer than 220 s, the pressing loads increase gradually and follow the same trend. Therefore, we can say that the minimum heating time in this case is 220 s. This result is completely consistent with the simulated results shown in Fig. 9. It should be pointed out that the sharp increase in pressing load at the early pressing stage may cause damages to the mold surfaces. In Fig. 11, the pressing loads approached the same level in the final stage, because heat transfer continued during pressing and the temperature in glass finally got uniform.

Another phenomenon caused by non-uniformity of temperature in glass is that the initially cylindrical glass preform, after pressing, will be deformed to be an isosceles trapezoid where the diameter of the bottom surface is bigger than that of the top surface. Fig. 12(a) shows an example of FEM simulated cross-sectional geometry with strain distribution of a glass piece pressed after a heating time of 180 s. The curvature radius of the upper corner is apparently larger than that of the lower corner. This is due to that the temperature of the upper surface was lower than that of the lower surface in the beginning of press, which caused a higher viscosity at the upper part. Although during pressing the heat transfer from the upper mold can finally eliminate the tem-

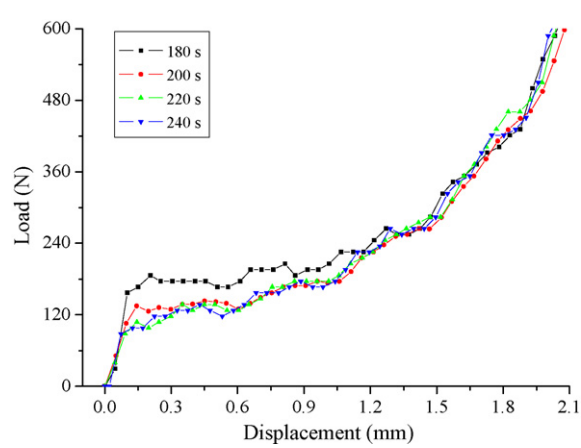

Fig. 11. Changes of pressing loads with time after heating for different soaking time.

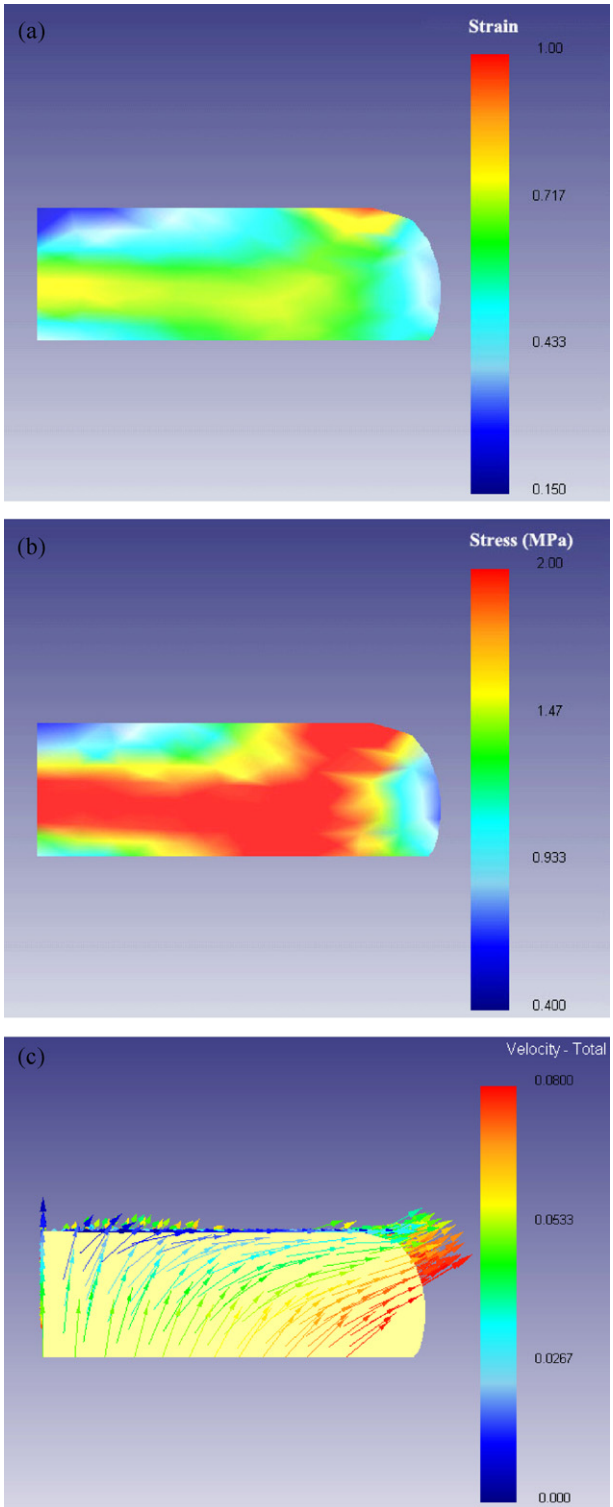

Fig. 12. FEM simulated results of (a) cross-sectional geometry with strain distribution, (b) equivalent stress distribution and (c) velocity distribution in the glass piece pressed after a heating time of 180 s.

perature difference, the deformation of the upper part has been delayed compared to the lower part. This effect finally led to the trapezoidal geometry of the glass piece. Similarly, in lens molding, non-uniformity of temperature will cause lens form error. Fig. 12(b) shows the equivalent stress (von Mises stress) distribution under the same condition as Fig. 12(a). The high-stress region is not symmetrical to the horizontal centerline but tends to be lower. This kind of stress distribution may cause deflection of the lens and non-uniformity in its optical properties. Fig. 12(c) shows an instantaneous velocity distribution of element nodes in glass at the end of the first press. It can be seen that near the symmetrical center,

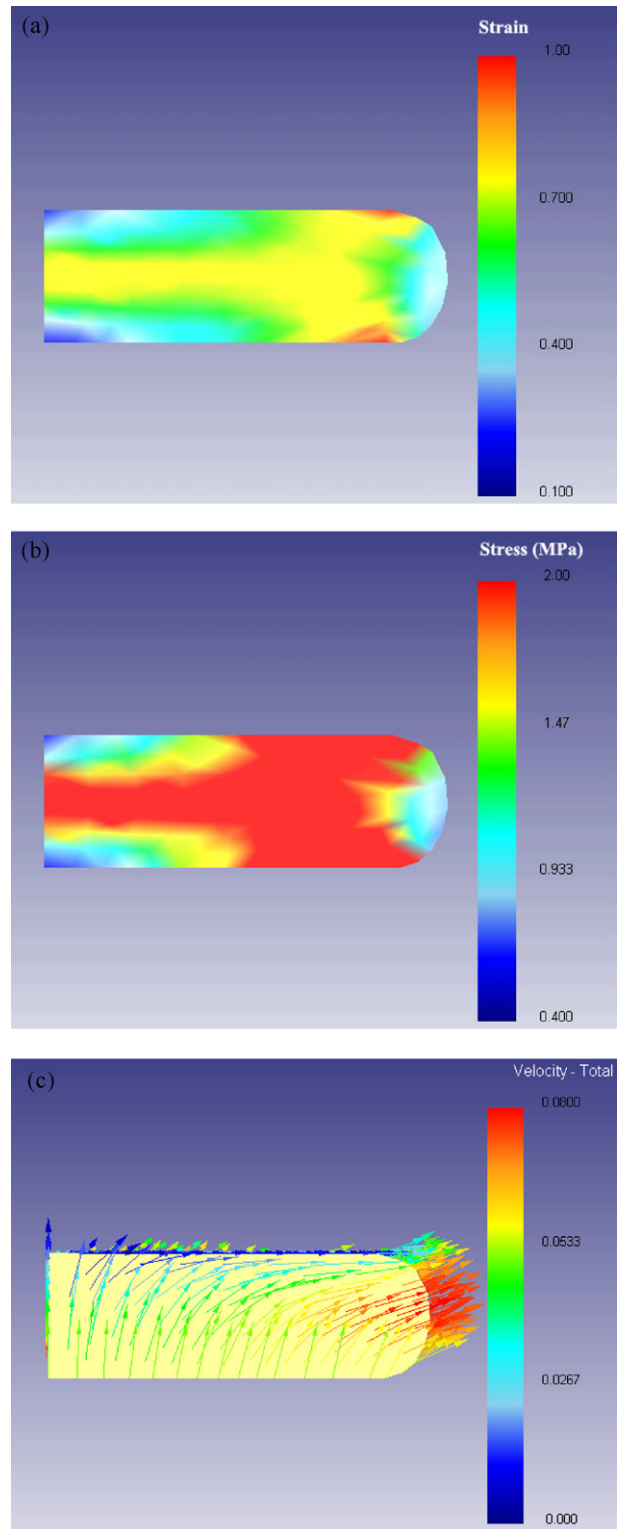

Fig. 13. FEM simulated results of (a) cross-sectional geometry with strain distribution, (b) equivalent stress distribution and (c) velocity distribution in the glass piece pressed after a heating time of 220 s.

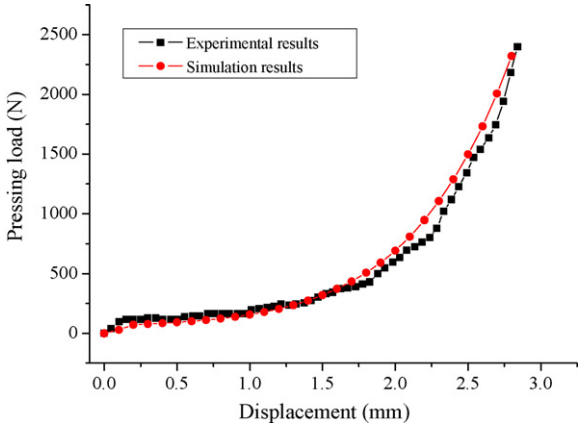

Fig. 14. Comparison between simulation results and experimental results of pressing load–displacement relationship.

velocity vectors are vertically directed; while in the outer region, material flow direction tends to be horizontal. It is also noteworthy that the material in the lower corner is completely stationary at this moment, and material flow can be found only in the upper region.

Fig. 13(a) is a simulated cross-sectional geometry with strain distribution of the glass piece pressed after a heating time of 220 s. In this case, the temperature within glass has become uniform. The curvature radius of the upper corner of the glass piece is completely the same as the lower corner. Fig. 13(b) shows the corresponding equivalent stress distribution. It is seen that the stress concentration region is basically symmetrical to the horizontal centerline. Fig. 13(c) shows the velocity distribution in glass at the end of the press. Obviously, velocity vector distribution in the outer region of the glass piece is very uniform, from the upper corner to the lower corner. From this point, we can say that choosing a suitable heating time is not only an important issue for prolonging the service life of molds, but also an essential step for improving form accuracy and optical property of the molded lenses.

Finally, pressing load was simulated based on the viscous deformation model discussed in Section 2. Fig. 14 shows the load change during pressing until the glass preform is pressed for a distance of 2.5 mm in the vertical direction (pressing rate = 3 mm/min, temperature = 590 °C). For comparison, experimentally measured pressing forces were also given in the figure. It can be seen that despite a small deviation between the experimental results and the simulated results at the beginning of pressing, which is presumably the effect of elastic deformation, the total trends of the results are basically the same.

5. Conclusions

High-temperature heat transfer and viscous deformation of glass in a lens molding process have been studied through theoretical analysis, experimental measurements and FEM simulations. The main results can be summarized as follows:

(1) A two-step pressing process is proposed for molding glass lenses. The first press is performed at a high temperature near the softening point to achieve most of the material deformation, and the second press is done at a low temperature between the yielding point and the transition point to finalize the lens geometry.
(2) Thermal expansion and heat transfer phenomena in glass molding process have been modeled by considering the temperature dependence of thermal properties of glass and interfacial conditions among glass, molds and environmental gas. The minimum heating time predicted by FEM simulation agrees well with the experimental results.
(3) High-temperature viscosity of glass near the softening point was measured by uniaxially pressing cylindrical glass preforms between a pair of flat molds on an ultraprecision glass molding machine, and the temperature-dependence of viscosity was clarified.
(4) Incomplete heating of glass not only causes sharp increase in pressing load at the beginning of pressing, but also leads to non-uniformity in viscous deformation and geometrical error of the glass component.
(5) High-temperature material flow of glass was simulated by a modified Newtonian fluid model, and the predicted pressing loads agree well with the experimental results.

Future work includes modeling of stress relaxation of glass during annealing and cooling to consolidate the foundations for simulating/visualizing a precision glass molding process for aspherical lenses, Fresnel lenses, DOEs and other surface microstructures.

Acknowledgements

The authors would like to thank Toshiba Machine Corporation for the technical supports in molding experiments. Thanks are also extended to Ohara Corporation for providing glass samples and technical data. This work has been supported by Japan Society for the Promotion of Science, Grant-in-Aid for Scientific Research (B), project number 19360055.

References

[1] Nicholas DJ, Boon JE. The generation of high precision aspherical surfaces in glass by CNC machining. Journal of Physics D: Applied Physics 1981: 593–600.
[2] Johnson RB, Michael M. Aspheric glass lens modeling and machining. In: Proceedings of SPIE, current developments in lens design and optical engineering VI. 2005. p. 58740B.
[3] Katsuki M. Transferability of glass lens molding. In: Proceedings of SPIE, 2nd International Symposium on advanced optical manufacturing and testing technologies. 2006. p. 61490M.
[4] Masuda J, Yan J, Kuriyagawa T. Application of the NiP-plated steel molds to glass lens molding. In: Proceedings of the 10th International Symposium on advances in abrasive technology. 2007. p. 123–30.
[5] Wakatsuki H, Satoh I. A study on separation behavior of press-molded glassware from a thermal engineering viewpoint: correlation of separation forces to the interface temperature between the mold and the glass. Heat Transfer-Asian Research 2001;30:660–75.
[6] Gakuroku S, Hachitani Y, Ikenishi M. Lens and its manufacturing method. Japan Patent No. 2007101585 (2007).
[7] Field RE, Viskanta R. Measurement and prediction of the dynamic temperature distributions in soda-lime glass plates. Journal of the American Ceramic Society 1990;73:2047–53.
[8] Wilson WRD, Schmid SR, Liu J. Advanced simulations for hot forging: heat transfer model for use with the finite element method. Journal of Materials Processing Technology 2004;155–156:1912–7.
[9] Viskanta R, Lim JM. Theoretical investigation of heat transfer in glass forming. Journal of the American Ceramic Society 2001;84:2296–302.
[10] Yi AY, Jain A. Compression molding of aspherical glass lenses—a combined experimental and numerical analysis. Journal of the American Ceramic Society 2005;88:579–86.
[11] Drotning WD. Thermal expansion of glasses in the solid and liquid phases. International Journal of Thermophysics 1985;6:705–14.
[12] Ohlberg SM, Woo TC. Thermal stress analysis of glass with temperature dependent coefficient of expansion. Rheologica Acta 1973;12:345–8.
[13] Choi J, Ha D, Kim J, Grandhi RV. Inverse design of glass forming process simulation using an optimization technique and distributed computing. Journal of Materials Processing Technology 2004;148:342–52.
[14] Zhou H, Li D. Mold cooling simulation of the pressing process in TV panel production. Simulation Modelling Practice and Theory 2005;13:273–85.
[15] Moser JB, Kruger OL. Thermal conductivity and heat capacity of the monophosphide and monosulfide of plutonium. Journal of the American Ceramic Society 1968;51:369–73.
[16] Richet P, Bottinga Y, Tequi C. Heat capacity of sodium silicate liquids. Journal of the American Ceramic Society 1984;67:C6–8.

[17] Sharp DE, Ginther LB. Effect of composition and temperature on the specific heat of glass. Journal of the American Ceramic Society 1951;34:260–71.
[18] Moore J, Sharp DE. Note on calculation of effect of temperature and composition on specific heat of glass. Journal of the American Ceramic Society 1958;41:461–3.
[19] Mann D, Field RE, Viskanta R. Determination of specific heat and true thermal conductivity of glass from dynamic temperature data. Heat and Mass Transfer 1992;27:225–31.
[20] McGraw DA. Transfer of heat in glass during forming. Journal of the American Ceramic Society 1961;44:353–63.
[21] Gent AN. Theory of the parallel plate viscometer. British Journal of Applied Physics 1960:85.
[22] Meister R. Parallel plate viscometer and its characteristic. In: Bulletin of the Research Institute of Mineral Dressing and Metallurgy, vol. 38. Tohoku University; 1982. p. 1–10.
[23] Fulcher GS. Analysis of recent measurements of the viscosity of glasses. Journal of the American Ceramic Society 1925;8:339–55.
[24] Kobayashi H, Takahashi H, Hiki Y. Temperature dependence of the viscosity through the glass transition in metaphosphate glasses and polystyrene. Materials Science and Engineering: 2006;442:263–7.
[25] Rouxel T, Huger M, Besson J. Rheological properties of Y–Si–Al–O–N glasses-elastic moduli, viscosity and creep. Journal of Materials Science 1992;27:279–84.
[26] Chang SH, Lee YM, Jung TS, Kang JJ, Hong SK, Shin GH, Heo YM. Simulation of an aspheric glass lens forming behavior in progressive GMP process. AIP Conference Proceedings 2007;908:1055–60.
[27] Li G, Jinn JT, Wu WT, Oh SI. Recent development and applications of three-dimensional finite element modeling in bulk forming processes. Journal of Materials Processing Technology 2001;113:40–5.
[28] Walters J, Wu W, Arvind A, Li G, Lambert D, Tang J. Recent development of process simulation for industrial applications. Journal of Materials Processing Technology 2000;98:205–11.
[29] Walters J, Kurtz S, Wu W, Tang J. The "State of the art" in cold forming simulation. Journal of Materials Processing Technology 1997;71:64–70.